2014-08

Two-body Förster resonance involving Rb nD states in a quasi-electrostatic trap

Two-body Förster resonance involving Rb nD states in a quasi-electrostatic trap

Jorge M. Kondo, Luis F. Gonçalves, Jader S. Cabral,[*] Jonathan Tallant, and Luis G. Marcassa[†]

Instituto de Física de São Carlos, Universidade de São Paulo, Caixa Postal 369, 13560-970, São Carlos, São Paulo, Brasil
(Received 9 May 2014; published 18 August 2014)

In this work, we excite $nD_{5/2}$ Rydberg states in a dense and cold Rb atomic sample held in a 10.6 μm quasi-electrostatic trap using narrow-bandwidth laser pulses. Our goal is to study the Förster resonance process $nD_{5/2} + nD_{5/2} \rightarrow (n-2)F + (n+2)P_{3/2}$ at zero electric field as a function of the total atomic density using pulsed-field ionization in the range $n = 37$–47. Such a process is almost degenerate for $n = 43$. Younge and coworkers studied this process [K. C. Younge, A. Reinhard, T. Pohl, P. R. Berman, and G. Raithel, Phys. Rev. A **79**, 043420 (2009)] and attributed the observed saturation to many-body effects. Our results show that as the ground-state atomic density increases, the $nD_{5/2}$ state population and the population transfer starts to saturate, which is consistent with the onset of Rydberg atom blockade and previously published results. However, since our experiment allows the independent measurement of the $nD_{5/2}$ and $(n+2)P_{3/2}$ state populations, we were able to obtain the $(n+2)P_{3/2}$ state population density dependence. Our results clearly show that the $(n+2)P_{3/2}$ state population depends quadratically on the total Rydberg atomic population, and consequently, the Förster resonance is a two-body process for a ground-state atomic density below 3×10^{11} cm^{-3}.

PACS number(s): 32.80.Ee, 34.50.Rk, 34.10.+x

I. INTRODUCTION

Many-body effects have been both a source of motivation as well as an explanation for experiments involving Rydberg atoms in ultracold trapped alkali gases since the beginning of this research field. Therefore, it is not surprising that the first seminal ultracold Rydberg results were interpreted as a manifestation of many-body interactions in the late 1990s [1,2]. Over the past ten years, several experimental results involving either Förster resonance or Rydberg atom blockade processes have been reported in the literature as a clear manifestation of many-body effects. Such works can be found in several recent reviews [3–7]. Most of the experimental results attributed to many-body effects in cold Rydberg atoms either involve the observation of excitation saturation effects or linewidth broadening in atomic samples held in a magneto-optical trap. Such association is done by comparing the experimental observations to complex theoretical models. These theoretical models are cumbersome due to the complexity of including many bodies. Thus, many-body models often rely on approximations to address the calculation, and a standard approximation involves breaking the problem into a series of two-body pieces. Therefore, the majority of the many-body models are based on the summation of Rydberg atom pair interactions [8,9], which make them computationally intense, and usually are limited to about 20 atoms.

It is important to point out that Förster resonance experiments are usually carried out in a magneto-optical trap at a maximum density on the order of 3×10^{10} cm^{-3}. To overcome this density limit, Reinhard and coworkers have loaded a single beam 1064-nm optical dipole trap to reach a maximum peak density of 5×10^{11} cm^{-3} for Rb [10]. The Rydberg states were excited using cw excitation with a resonant two-photon process. In a later experiment, the same group studied the

$43D_{5/2} + 43D_{5/2} \rightarrow 41F + 45P_{3/2}$ Förster resonance in an optical dipole trap [11]. To explain a saturation effect on the population transfer in the Förster resonance, the authors have used a complete basis many-body theory (CBMBT) simulation, which can account for the N-body Rydberg state exchange dynamics from coherent mixtures of D, P, and F components. Although, the theoretical model was able to explain their results, the authors did not explore the atomic density dependence of the $43D_{5/2}$ and $45P_{3/2}$ state populations.

In this work, our goal is to independently measure the atomic density dependence of $nD_{5/2}$ and $(n+2)P_{3/2}$ state populations using pulsed-field ionization in the $n = 37$–47 range, complementing the work done by Younge and coworkers [11]. We excite $nD_{5/2}$ Rydberg states in a dense and cold Rb atomic sample held in a quasi-electrostatic trap using narrow-bandwidth laser pulses. In this way we can study the $nD_{5/2} + nD_{5/2} \rightarrow (n-2)F + (n+2)P_{3/2}$ process at zero electric field, which is almost degenerate for $n = 43$. We have observed that as the ground state atomic density increases, the $nD_{5/2}$ state population and the population transfer start to saturate, which is consistent with the onset of Rydberg atom blockade and previous results [11]. Younge and coworkers have associated the saturation of the population transfer to many-body effects [11]. Our results show that the $(n+2)P_{3/2}$ state population exhibits similar behavior. However, the population depends quadratically on the total Rydberg atomic population, indicating that the transfer mechanism is a two-body process for a ground-state atomic density below 3×10^{11} cm^{-3}. The result is contradictory to the interpretation proposed by Younge and coworkers [11], suggesting that a two-body process can also exhibit saturation effects.

II. EXPERIMENTAL SETUP

Our magneto-optical trap (MOT) operates in a stainless steel chamber with a background pressure below 10^{-10} torr, and it is loaded from an atomic vapor provided by an Rb dispenser. We start from a standard MOT, which traps about 5×10^7 ^{85}Rb atoms at an atomic density of $\sim 10^{10}$ cm^{-3}. The

———————
[*]Present Address: Instituto de Física, Universidade Federal de Uberlândia, Caixa Postal 593, 38400-902, Uberlândia, Minas Gerais, Brasil.
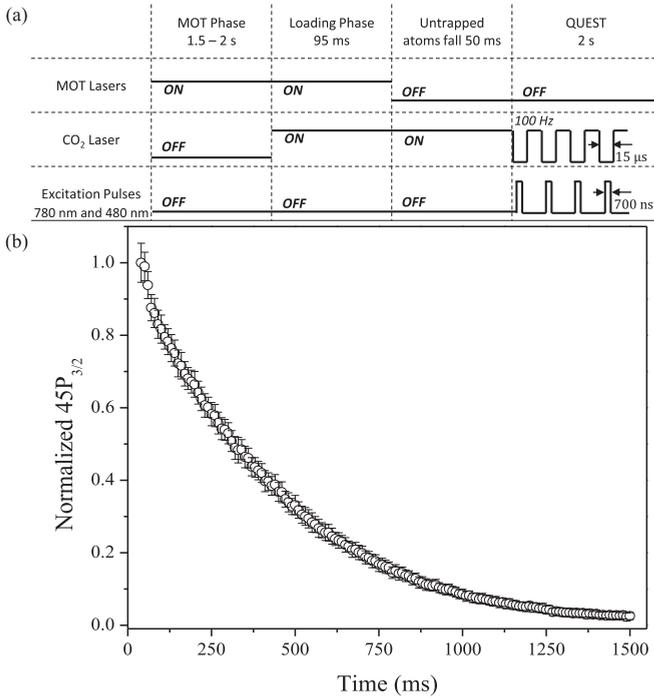[†]marcassa@ifsc.usp.br

(a)

(b)

FIG. 1. (a) Experimental time sequence. The QUEST phase may be varied up to 2 s. (b) Typical $45P_{3/2}$ signal obtained as a function of QUEST decay time using a boxcar gate.

trapping laser beam is tuned to the red of the $5S_{1/2}(F = 3) \rightarrow 5P_{3/2}(F' = 4)$ atomic transition and the repumping laser beam is resonant with the $5S_{1/2}(F = 2) \rightarrow 5P_{3/2}(F' = 3)$ atomic transition. At the MOT conditions, the trapping laser intensity per arm is $I_T = 6$ mW cm^{-2} and detuning is $\Delta_T \simeq -2.7\Gamma$, where $\Gamma = 2\pi \times 6.1$ MHz; the repumping laser intensity per arm is $I_R \simeq 0.9$ mW cm^{-2} and with a detuning $\Delta_R = 0$. The repumping frequency is obtained using an electro-optical modulator (EOM). The quasi-electrostatic trap (QUEST) is provided by a polarized 10.6-μm CO$_2$ laser (COHERENT model GEM-100), which is focused into the MOT volume with a waist of 35 μm at an available power of 80 W. The calculated trap depth is about 2.5 mK.

The experiment runs according to the time sequence shown in Fig. 1(a). (i) A MOT loading phase, whose duration is about 1.5–2 s, consisting of both trapping and repumping laser beams at the initial MOT conditions. The QUEST remains off. (ii) A QUEST loading phase, whose duration is 95 ms. In this phase, the QUEST beam is turned on and the intensity and frequency of the MOT lasers are varied to loading conditions ($I_T = 1.2$ mW cm^{-2}, $\Delta_T \simeq -6.8\Gamma$, $I_R \simeq 60$ μW cm^{-2}, and $\Delta_R = -4\Gamma$). At the end of this phase we apply a 100-μs pulse of the repumping laser beam at an intensity of $I_R \simeq 250$ μW cm^{-2}, which allows us to optically pump the atoms to the $F = 3$ hyperfine ground state. (iii) Finally, the untrapped atoms are allowed to fall under gravity for 50 ms, so at the end of this phase we have a nonpolarized atomic sample held in the QUEST with about 10^6 atoms at a density of $3.0 \pm 0.7 \times 10^{11}$ cm^{-3} and a temperature of 80 μK. (iv) In the sequence, we apply a laser pulse train to excite the Rydberg states, which are subsequently detected by pulsed-field ionization (PFI). This laser pulse train operates at 100 Hz for 2 s and it is composed

of two narrow-bandwidth cw laser pulses near 780 and 480 nm, whose duration is about 700 ns and have intensities of $I_{780} = 1.6$ mW cm^{-2} and $I_{480} = 80$ W cm^{-2} (Rabi frequency of 18.5 MHz). The PFI occurs 70 ns after the optical excitation. The QUEST is turned off for about 15 μs during the Rydberg excitation and detection to avoid any unwanted effects such as ac Stark shifts or photoionization of the Rydberg states [12]. During the laser pulse train, the atomic population held in the QUEST decays, allowing us to study the nD Rydberg-state excitation and the $(n + 2)P$ state population transfer as a function of the ground-state atomic density. To characterize the sample's decay, a state-selective absorption imaging technique was used. The background electric field is estimated to be <20 mV cm^{-1}. It was also verified that the laser pulse train does not appreciably affect the trap lifetime. Two boxcar gates are used to selectively detect the nD and $(n + 2)P$ electron signals to study the population transfer process in the range $n = 37$–47. Such signals are obtained as a function of QUEST decay time. Typical $45P_{3/2}$ electron signal data are shown in Fig. 1(b). Using the absorption images we are able to convert the time scale into ground-state atomic density.

III. RESULTS AND DISCUSSION

To analyze our experimental data, we have used a state-mixing fraction similar to the one introduced by Younge and coworkers [11], which they obtained by fitting their electron signal. However, since we used boxcar gates, we have defined our state-mixing fraction as twice the $(n + 2)P$ electron signal divided by the sum of the nD electron signal plus the $(n + 2)P$ electron signal. The fraction is defined in this way because it is very possible that the $(n - 2)F$ electron signal may contaminate the nD electron signal since the $(n - 2)F$ states ionize over a large range of electric field [13]. A typical density dependence measurement of the state-mixing fraction is shown in Fig. 2(a) for the $43D_{5/2}$ state. Each point is the average of ten measurements and the standard deviation is the reported error. Although the absolute value of the state-mixing fraction is different than in Ref. [11], the qualitative behavior is the same. Such a quantitative difference may be due to stimulated emission because we have a higher Rabi frequency and a longer excitation time. Another possibility is the fact that our sample is really a three-dimensional sample with about 2×10^4 Rydberg atoms in contrast to the small sample, about 15 Rydberg atoms, used by Younge and coworkers [11]. Differences due to dimensionality have already been reported in the literature [14]. Figure 2(a) clearly presents a saturation as the atomic density increases, similar to the behavior observed by the authors of Ref. [11]. In addition to the $43D_{5/2}$ electron signal, the same behavior is also observed for the $45P_{3/2}$ electron signal, as shown in Fig. 2(b). We should point out that in this figure we have normalized the sum of the $43D_{5/2}$ and $45P_{3/2}$ electron signals at maximum atomic density. The state-mixing fraction and the $nD_{5/2}$ and $(n + 2)P_{3/2}$ electron signals present the same qualitative behavior for the entire $n = 37$–47 range.

The observed atomic density dependence of the nD electron signal can be explained by the Rydberg atom blockade effect, which has been extensively studied both theoretically and experimentally in the last decade [3–7]. Briefly, if we consider two atoms separated by an internuclear distance R, the
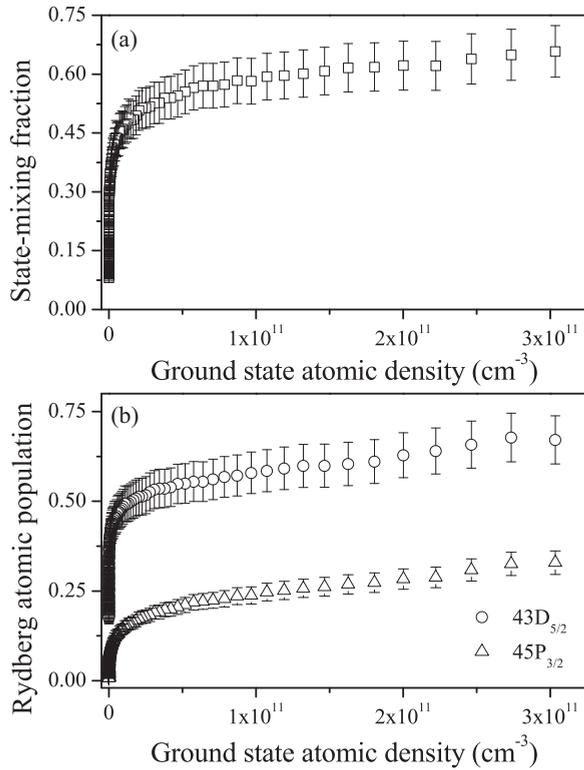
FIG. 2. (a) State-mixing fraction of the $43D_{5/2}$ state and (b) $43D_{5/2}$ and $45P_{3/2}$ populations as function of the ground-state atomic density.

Rydberg excitation of one atom will depend on the excitation of the other due to the fact that the energy level is shifted by the interaction, detuning it from the excitation laser. The result is that in a given volume, there is a limit on the number of Rydberg atoms that can be excited, thereby leading to a saturation of the excitation. This effect was first proposed for a pair of atoms but can also be observed in a large ensemble of cold atoms [15]. In a large ensemble, the Rydberg excitation is shared collectively between all the atoms within the range of the distance over which the energy shift between two atoms causes the excitation to be blocked. The range over which a second excitation in the ensemble can be blocked is called the blockade radius. The saturation of the excitation was observed in several experiments [10,16–18], and later it was theoretically modeled [19,20]. To demonstrate that our $43D$ results are consistent with Rydberg atom blockade, we have fit the data to a classical hard sphere model in the steady state (dashed line in Fig. 3) [21,22]. This is the simplest model available in the literature, but it does contain the main physical insights and correctly describes the effect. Briefly, the hard sphere model treats Rydberg atoms as hard spheres with a radius equal to the blockade radius thereby defining an exclusion volume around each excited atom. The excitation volume is assumed to be densely packed by these spheres so that information about the excited state population is obtained. We should point out that the fit deviates at higher densities since this model does not take into account population transfer to the $(n+2)P$ state. The focus of the present work is not to study the Rydberg atom blockade, however, from such a fit we obtain a blockade radius of about 4 μm for the $43D_{5/2}$ state, which
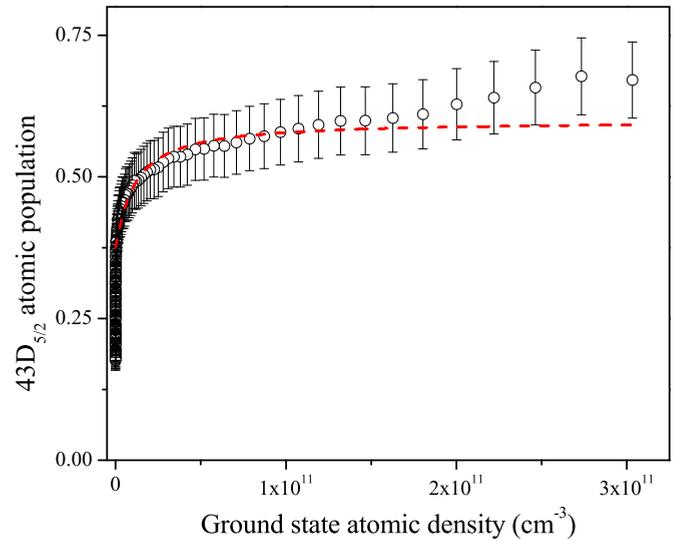

FIG. 3. (Color online) $43D_{5/2}$ population as a function of the ground-state atomic density. The dashed (red) line is obtained from a theoretical classical hard sphere model in the steady state [21,22]. From this fit, we obtain a blockade radius of about 4 μm for the $43D_{5/2}$ state.

is consistent with present measurements [23,24]. This assures us that the observed density dependence for the excitation of the $43D_{5/2}$ state is due to Rydberg atom blockade.

The next step in our analysis is to plot the $(n+2)P$ population as a function of the total Rydberg atomic population $[nD + (n+2)P]$. If many-body effects are important in our experiment, as suggested by Younge and coworkers [11], such a plot should show it explicitly. Recently, this analysis was used by Gurian and coworkers to clearly identify a four-body Förster resonance process in Cs [25]. They have shown that the atomic $23D_{5/2}$ population scales as the fourth power of
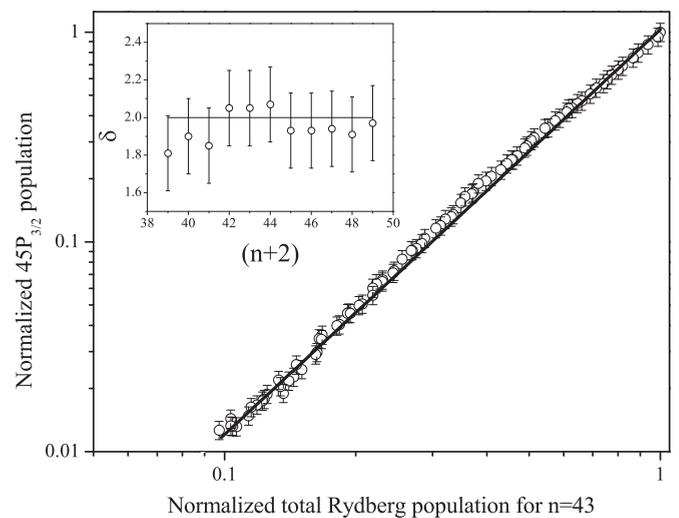

FIG. 4. Normalized $45P_{3/2}$ population as a function of the normalized total Rydberg atomic population for $n = 43$. The full line is a power-law fit to the total Rydberg atom density at $n = 43$, ρ_{43}^{δ}, where δ is a fitting parameter. The fit gives $\delta = 1.9 \pm 0.2$. The inset shows δ as a function of $(n+2)$, the full line is obtained considering a two-body interaction.

the total Rydberg atomic density, which is a clear signature of a multiparticle effect. The authors have also shown that a Förster resonance previously attributed to many bodies is, in fact, due to a two-body process [2]. In Fig. 4, we show a typical normalized $45P_{3/2}$ population as a function of the normalized total Rydberg atomic population for $n = 43$. The symbols are the experimental data and the line is a power-law fit to the total Rydberg atom density for $n = 43$, ρ_{43}^δ, where δ is a fitting parameter. The fit gives $\delta = 1.9 \pm 0.2$. In the inset of Fig. 4, we show δ as a function of $(n + 2)$. By comparing to the experimental results, it is clear that even at our highest atomic density, the observed Förster resonance process is due to a two-body effect. It is worth mentioning that the density region where we have observed saturation represents experimental points for a normalized total Rydberg atomic population above 0.6. Therefore, the saturation effect observed for the state-mixing fraction in Fig. 2(a) is just due to saturation of the excitation of the $43D_{5/2}$ state, which is caused by the Rydberg atom blockade effect. The population transfer process itself does not present any saturation.

IV. CONCLUSION

We have studied the Förster resonance process $nD_{5/2} + nD_{5/2} \rightarrow (n - 2)F + (n + 2)P_{3/2}$ at zero electric field for the $n = 37$–47 range using a dense atomic sample held in a quasi-electrostatic trap. The atomic density dependence of the $nD_{5/2}$ state population exhibited a saturation effect, which was shown to be due to the Rydberg atom blockade effect, in accordance with previous results. Although the $(n + 2)P_{3/2}$ state population presented similar behavior, we have demonstrated that the transfer process itself exhibits no saturation. In addition, we have clearly shown that the $(n + 2)P_{3/2}$ population depends quadratically on the total Rydberg atom population, indicating that the Förster resonance is a two-body process for a ground-state atomic density below 3×10^{11} cm^{-3}. This result is contradictory to the interpretation proposed by Younge and coworkers [11], suggesting a two-body process can also exhibit saturation effects. In conclusion, the observation of saturation effects can not be linked to many-body effects in a straightforward way.

[1] W. R. Anderson, J. R. Veale, and T. F. Gallagher, Phys. Rev. Lett. **80**, 249 (1998).

[2] I. Mourachko, D. Comparat, F. de Tomasi, A. Fioretti, P. Nosbaum, V. M. Akulin, and P. Pillet, Phys. Rev. Lett. **80**, 253 (1998).

[3] M. Saffman, T. G. Walker, and K. Mølmer, Rev. Mod. Phys. **82**, 2313 (2010).

[4] R. Löw, H. Weimer, J. Nipper, J. B. Balewski, B. Butscher, H. P. Büchler, and T. Pfau, J. Phys. B **45**, 113001 (2012).

[5] D. Comparat and P. Pillet, J. Opt. Soc. Am. B **27**, A208 (2010).

[6] T. F. Gallagher and P. Pillet, in *Advances in Atomic, Molecular, and Optical Physics*, Vol. 56, edited by E. Arimondo *et al.* (Academic, New York, 2008), p. 161.

[7] L. G. Marcassa and J. P. Shaffer, in *Advances in Atomic, Molecular, and Optical Physics*, edited by E. Arimondo *et al.* (Academic, New York, 2014).

[8] J. V. Hernandez and F. Robicheaux, J. Phys. B **39**, 4883 (2006).

[9] B. Sun and F. Robicheaux, Phys. Rev. A **78**, 040701 (2008).

[10] A. Reinhard, K. C. Younge, and G. Raithel, Phys. Rev. A **78**, 060702 (2008).

[11] K. C. Younge, A. Reinhard, T. Pohl, P. R. Berman, and G. Raithel, Phys. Rev. A **79**, 043420 (2009).

[12] J. Tallant, D. Booth, and J. P. Shaffer, Phys. Rev. A **82**, 063406 (2010).

[13] T. F. Gallagher, *Rydberg Atoms*, 1st ed. (Cambridge University Press, Cambridge, England, 1994).

[14] T. J. Carroll, S. Sunder, and M. W. Noel, Phys. Rev. A **73**, 032725 (2006).

[15] M. D. Lukin, M. Fleischhauer, R. Cote, L. M. Duan, D. Jaksch, J. I. Cirac, and P. Zoller, Phys. Rev. Lett. **87**, 037901 (2001).

[16] D. Tong, S. M. Farooqi, J. Stanojevic, S. Krishnan, Y. P. Zhang, R. Côté, E. E. Eyler, and P. L. Gould, Phys. Rev. Lett. **93**, 063001 (2004).

[17] K. Singer, M. Reetz-Lamour, T. Amthor, L. G. Marcassa, and M. Weidemüller, Phys. Rev. Lett. **93**, 163001 (2004).

[18] R. Heidemann, U. Raitzsch, V. Bendkowsky, B. Butscher, R. Löw, L. Santos, and T. Pfau, Phys. Rev. Lett. **99**, 163601 (2007).

[19] C. Ates, T. Pohl, T. Pattard, and J. M. Rost, Phys. Rev. A **76**, 013413 (2007).

[20] A. Chotia, M. Viteau, T. Vogt, D. Comparat, and P. Pillet, New J. Phys. **10**, 045031 (2008).

[21] M. Robert-de-Saint-Vincent, C. S. Hofmann, H. Schempp, G. Günter, S. Whitlock, and M. Weidemüller, Phys. Rev. Lett. **110**, 045004 (2013).

[22] C. Ates, S. Sevinçli, and T. Pohl, Phys. Rev. A **83**, 041802 (2011).

[23] A. Schwarzkopf, R. E. Sapiro, and G. Raithel, Phys. Rev. Lett. **107**, 103001 (2011).

[24] A. Schwarzkopf, D. A. Anderson, N. Thaicharoen, and G. Raithel, Phys. Rev. A **88**, 061406 (2013).

[25] J. H. Gurian, P. Cheinet, P. Huillery, A. Fioretti, J. Zhao, P. L. Gould, D. Comparat, and P. Pillet, Phys. Rev. Lett. **108**, 023005 (2012).